CrossMark

SPECIAL

A. Ganczarski · D. Szubartowski

Plane stress state of FGM thick plate under thermal loading

Abstract This paper demonstrates the plane stress state of FGM thick plate under thermal loading. First, the Sneddon–Lockett theorem on the plane stress state in an isotropic infinite thick plate is generalized for a case of FGM problem in which all thermomechanical properties are optional functions of depth coordinate. Next, an example of application to an engineering problem is presented.

Keywords FGM thick plate · Plane stress state · Thermal loading

1 Introduction

Functionally graded materials (FGMs) provide thermal insulation and mechanical toughness at high temperature by varying the composition of thermal conductivity coefficient, thermal expansion coefficient and Young's modulus from high-temperature side to low-temperature side continuously and simultaneously by removing the discontinuity of layered plate. These advantages cause that FGMs are applicable in many fields such as high-performance engines for aerospace vehicles, turbine blades and heat-resisting tools. A general overview of thermal stresses in FGMs comprises work by Noda [1].

Numerous analytical solutions of thermoelastic plane or three-dimensional problems of FGMs take advantage of specific power or exponential function approximation methods of multilayered composite plate, limiting simultaneously their generality and suggesting question how to reduce the problem. One way to attain this may be generalization of theorem on the plane stress state in an isotropic thermoelastic thick plate proved by Sneddon and Lockett in [2]. The authors presented convinced proof for a problem of semi-infinite thermoelastic medium bounded by two parallel planes and loaded by an arbitrary temperature field on one surface. The method of solution employed was the double Fourier transforms. The results confirmed solution of analogous problems, being inspiration to their work, received earlier by Sternberg and McDowell [3], based on Green's function, and by Muki [4], who used method combining the theory of Fourier series and the Hankel transforms of integral order.

Recent achievements concerning application of FGM layer, treated directly as thermal barrier coating or indirectly as interface between coating and substrate, are mainly focused on plates or shells of thin or moderate thickness in which assumptions of plane stress or simplified 3D stress states are natural consequences of Kirchhoff–Love's or Reissner–Mindlin's hypotheses used. Contrary to aforementioned broad stream of papers,

A. Ganczarski (✉) · D. Szubartowski
Department of Mechanical Engineering, Institute Applied Mechanics, Cracow University of Technology,
Al. Jana Pawła II 37, 31-864 Kraków, Poland
E-mail: artur@cut1.mech.pk.edu.pl; artur.ganczarski@pk.edu.pl

D. Szubartowski
E-mail: tszubartowski@o2.pl

the number of works concerning fully 3D problems, like thick plate or semi-space, is rather limited. Hence, let us mention several of them in chronological order.

Senthil and Batra [5] analyze 3D thermomechanical deformation of simply supported rectangular plate subjected to instantaneous temperature. Authors use Laplace's transformation technique to reduce uncoupled quasi-static equations of linear thermoelasticity to an ordinary differential equations containing the power-law-type functions of effective thermomechanical constants. Magnitudes of these constants (bulk and shear moduli, coefficients of thermal conductivity and expansion) at a point are determined according to either the Mori–Tanaka or self-consistent scheme and directly depend on from volume fraction of constituents (Al/SiC). The following results for plates, subjected to either time-dependent temperature or heat flux prescribed on top surface, are demonstrated at several critical locations: transient temperature, displacements and thermal stresses.

Dai et al. [6] present a mesh-free model applied to the active shape control as well as the dynamic response of plate containing piezoelectric sensors and actuators. Authors consider FGM plate made of ceramics (Zirconia) and metal (Al) for which volume fraction varies continuously in thickness direction according to a power law. The element-free Galerkin method is applied do derive shape functions which next serve to study several numerical (FEM) examples.

Transversely isotropic, piezoelectric FGM half-space problem is reported by Pan and Han [7]. Authors introduce original concept of functionally graded Green's functions for better capturing of nature of displacement, stress and electric potential fields corresponding to functionally a graded PZT-4 half-space and a coated functionally graded PZT-4 layer over a homogeneous BaTiO$_3$ half-space. This work can be treated as excellent extension of paper by Sternberg and McDowell [3] since under certain assumptions there exists fully analogy between fields of electric potential and temperature.

Problem of functionally graded half-space under steady point heat source is analyzed by Wang et al. [8]. Authors derived three-dimensional Green's functions in order to describe thermal conductivity, which varies exponentially along arbitrary direction. Except the case mentioned in title, three other cases are considered: temperature field in functionally graded full-space induced by a moving point heat source, electric potential due to static point electric charge in a dielectric full-space and 2D time-harmonic dynamic Green's function for FGM.

An exact solution of steady-state thermoelastic problem of 3D circular FGM plate under thermal and mechanical loads is presented by Jabbari et al. [9]. Material properties, except Poisson's ratio, are assumed to varying exponentially across the thickness direction. Assuming axial symmetry of the problem, authors present exact analytical solution concerning: temperature distribution, displacement and stress components, for metal Ti–6Al–4V and ceramic ZrO$_2$ FGM.

Yang et al. [10] present the new approach for 2D and 3d thermal stress analysis of FGMs by use of analytical expressions in radial integration boundary element method. Application of Kelvin's fundamental solutions leads to integral equations which include both non-homogeneity and temperature variations of the material. Next, integrals are transformed into equivalent boundary integrals using RIBEM. Authors demonstrate efficiency of presented approach inserting: temperature, displacement and stress distributions of exemplary hexahedral structure. Presented BEM-based method is competitive to conventional FEM-based methods since it allows to save more than 60 % of computational time.

Kulikov and Plotnikova [11] present a new method of sampling surfaces (SaS) applied to 3D steady-state problem of laminated FGM plates subjected to thermomechanical loading. This method is based on choosing inside each laminate layer the sampling surfaces such that temperature and displacements of these surfaces are basic plate variables. Above concept allows to present the thermoelastic laminated FG plate formulation in a very compact form. Since sampling surfaces are located inside each layer at Chebyshev's polynomial nodes, the uniform convergence of the method is guaranteed. Two exemplary solutions are demonstrated: temperature, heat flux and displacements for metal/ceramic (Al/SiC) square plate and temperature, heat flux, displacements and stresses for graphite/epoxy square plate covered with metal/ceramic barrier on its top surface.

2 The general solution of FGM thermoelastic problem

A thermoelastic three-layer body under consideration (Fig. 1) is bounded by two parallel planes normal to axis x_3, and its FGM interface thermomechanical properties such as thermal conductivity coefficient, thermal expansion coefficient and Young's (Kirchhoff's) modulus are optional functions of x_3

$$\lambda = \lambda(x_3), \quad \alpha = \alpha(x_3), \quad E = E(x_3), \quad G = G(x_3). \tag{1}$$
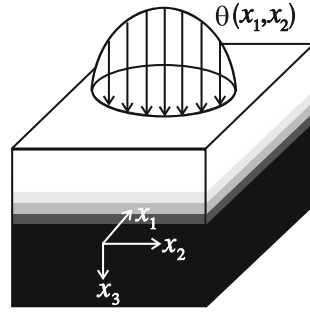
Fig. 1 Thick thermoelastic body with FGM interface under optional thermal load

The body is established a temperature field $T + \theta(x)$, where T in the temperature of the solid corresponding to zero stress and strain. Also, it is assumed that there are no body forces within the solid and that its surfaces are free from tractions.

The system of equations of uncoupled thermoelasticity takes the form

$$\nabla^2 u_i + \frac{1}{1-2\nu}\frac{\partial \Theta}{\partial x_i} + \underline{\frac{1}{G}\frac{\partial G}{\partial x_3}\left(\frac{\partial u_i}{\partial x_3} + \frac{\partial u_3}{\partial x_i}\right)} = 2\frac{1+\nu}{1-2\nu}\frac{\partial(\alpha\theta)}{\partial x_i}$$

$$\nabla^2 u_3 + \frac{1}{1-2\nu}\frac{\partial \Theta}{\partial x_3} + \underline{\frac{2}{G}\frac{\partial G}{\partial x_3}\left(\frac{\partial u_3}{\partial x_3} + \frac{\nu\Theta}{1-2\nu}\right)} = 2\frac{1+\nu}{1-2\nu}\left[\frac{\partial(\alpha\theta)}{\partial x_3} + \underline{\frac{1}{E}\frac{\partial E}{\partial x_3}\alpha\theta}\right]$$

$$\nabla^2 \theta + \underline{\frac{1}{\lambda}\frac{\partial \lambda}{\partial x_3}\frac{\partial \theta}{\partial x_3}} = 0 \tag{2}$$

where u_i denotes the displacement vector, $\Theta = \text{div}(u_i)$ is the dilatation and ν stands for Poisson's ratio (independent of x_3). The underlined terms in Eq. (2) yield of FGM application, and they are additional one in comparison with classical formulation of homogeneous material. The variation of temperature θ throughout the solid is determined by steady Fourier equation Eq. (2_3) in case of absence of inner heat sources. The relation between the stress tensor σ_{ij} and the displacement vector u_i is given by the Duhamel–Neumann equation

$$\sigma_{ij} = G\left[\frac{\partial u_i}{\partial x_j} + \frac{\partial u_j}{\partial x_i} + 2\left(\frac{\nu(\Theta - 3\alpha\theta)}{1-2\nu} - \alpha\theta\right)\delta_{ij}\right] \tag{3}$$

To solve Eq. (2), the following potential, originally proposed by Iljushin et al. [12], is introduced

$$u_i = \frac{\partial \phi}{\partial x_i} \quad i = 1, 2, \quad f(x_3) = Ax_3^2 + Bx_3 + C$$

$$u_3 = -\frac{\partial \phi}{\partial x_3} + f(x_3), \quad \alpha\theta = 2\frac{1-\nu}{1+\nu}Ax_3 - \frac{1}{1+\nu}\frac{\partial^2 \phi}{\partial x_3^2} \tag{4}$$

where function of displacement potential ϕ is of harmonic type

$$\nabla^2 \phi = 0 \tag{5}$$

and A, B, and C are constants.

Simple introducing of definitions (4) to Eq. (2) shows that only equations of mechanical state are satisfied as identity

$$\frac{\partial}{\partial x_i}\underbrace{(\nabla^2 \phi)}_{=0} + \frac{1}{1-2\nu}\frac{\partial}{\partial x_i}\left(\underbrace{\nabla^2 \phi}_{=0} - 2\frac{\partial^2 \phi}{\partial x_3^2} + \frac{\partial f}{\partial x_3}\right)$$

$$+ \frac{1}{G}\frac{\partial G}{\partial x_3}\left(\underbrace{\frac{\partial^2 \phi}{\partial x_3 \partial x_i} - \frac{\partial^2 \phi}{\partial x_i \partial x_3}}_{=0}\right) = 2\frac{1+\nu}{1-2\nu}\left(-\frac{1}{1+\nu}\frac{\partial^3 \phi}{\partial x_i \partial x_3^2}\right)$$

$$-\frac{\partial}{\partial x_3}\underbrace{(\nabla^2\phi)}_{=0} + \frac{\partial^2 f}{\partial x_3^2} + \frac{1}{1-2\nu}\frac{\partial}{\partial x_3}(\underbrace{\nabla^2\phi}_{=0} - 2\frac{\partial^2\phi}{\partial x_3^2} + \frac{\partial f}{\partial x_3})$$

$$+\frac{2}{G}\frac{\partial G}{\partial x_3}[-\frac{\partial^2\phi}{\partial x_3^2} + \frac{\partial f}{\partial x_3} + \frac{\nu}{1-2\nu}(\underbrace{\nabla^2\phi}_{=0} - 2\frac{\partial^2\phi}{\partial x_3^2} + \frac{\partial f}{\partial x_3})]$$

$$= 2\frac{1+\nu}{1-2\nu}\left[2\frac{1-\nu}{1+\nu}A - \frac{1}{1+\nu}\frac{\partial^3\phi}{\partial x_3^3} + \frac{1}{E}\frac{\partial E}{\partial x_3}\left(2\frac{1-\nu}{1+\nu}Ax_3 - \frac{1}{1+\nu}\frac{\partial^3\phi}{\partial x_3^3}\right)\right] \tag{6}$$

if only $B = 0$ and $\frac{1}{G}\frac{\partial G}{\partial x_3} = \frac{1}{E}\frac{\partial E}{\partial x_3}$, which is true for $\nu = $ const, contrary to the case of homogeneous material when also the equation of thermal state is satisfied as identity.

The stress components referring to the plane stress state with respect to axis x_3

$$\sigma_{i3} = G\left(\frac{\partial u_i}{\partial x_3} + \frac{\partial u_3}{\partial x_i}\right) = G(\underbrace{\frac{\partial^2\phi}{\partial x_i\partial x_3} - \frac{\partial^2\phi}{\partial x_3\partial x_i}}_{=0}) = 0,$$

$$\sigma_{33} = 2G\left[\frac{\partial u_3}{\partial x_3} - \alpha\theta + \frac{\nu(\Theta - 3\alpha\theta)}{1-2\nu}\right] = 2G\left\{-\frac{\partial^2\phi}{\partial x_3^2} + \frac{\partial f}{\partial x_3}\right.$$

$$-2\frac{1-\nu}{1+\nu}Ax_3 + \frac{1}{1+\nu}\frac{\partial^2\phi}{\partial x_3^2} + \frac{\nu}{1-2\nu}\left[\underbrace{\nabla^2\phi}_{=0} - 2\frac{\partial^2\phi}{\partial x_3^2} + \frac{\partial f}{\partial x_3}\right.$$

$$\left.\left.-3\left(2\frac{1-\nu}{1+\nu}Ax_3 - \frac{1}{1+\nu}\frac{\partial^2\phi}{\partial x_3^2}\right)\right]\right\} = 2G\frac{1-\nu}{1-2\nu}B \tag{7}$$

are also identically equal to zero when $B = 0$ for any point x_i, what ends the proof. It is interesting to note that application of Eq. (4) transforms original mechanical problem Eq. (2₁), which involves material non-homogeneity, into mechanically homogeneous one

$$\overline{\nabla}^2\phi + 2(1-\nu)Ax_3 - (1+\nu)\alpha\theta = 0,$$
$$\nabla^2\theta + \frac{1}{\lambda}\frac{\partial\lambda}{\partial x_3}\frac{\partial\theta}{\partial x_3} = 0, \tag{8}$$

where $\overline{\nabla}^2 = \frac{\partial^2}{\partial x_1^2} + \frac{\partial^2}{\partial x_2^2}$.

It is obvious that the Iljushin potential (4) rewritten to the form suitable for axial symmetry $x_1 = r$, $x_3 = z$, $u_1 = u$ and $u_3 = w$

$$u = \frac{\partial\phi}{\partial r}, \quad f(z) = Az^2 + Bz + C$$

$$w = -\frac{\partial\phi}{\partial z} + f(z), \quad \alpha\theta = 2\frac{1-\nu}{1+\nu}Az - \frac{1}{1+\nu}\frac{\partial^2\phi}{\partial z^2} \tag{9}$$

satisfies as identity the two first equations of following system

$$\nabla^2 u + \frac{1}{1-2\nu}\frac{\partial\Theta}{\partial r} + \frac{1}{G}\frac{\partial G}{\partial z}\left(\frac{\partial r}{\partial z} + \frac{\partial w}{\partial r}\right) = 2\frac{1+\nu}{1-2\nu}\frac{\partial(\alpha\theta)}{\partial r}$$

$$\nabla^2 w + \frac{1}{1-2\nu}\frac{\partial\Theta}{\partial z} + \frac{2}{G}\frac{\partial G}{\partial z}\left(\frac{\partial w}{\partial z} + \frac{\nu\Theta}{1-2\nu}\right) = 2\frac{1+\nu}{1-2\nu}\left[\frac{\partial(\alpha\theta)}{\partial z} + \frac{1}{E}\frac{\partial E}{\partial z}\alpha\theta\right]$$

$$\nabla^2\theta + \frac{1}{\lambda}\frac{\partial\lambda}{\partial z}\frac{\partial\theta}{\partial z} = 0 \tag{10}$$

as well as the stress components referring to the z axis

$$\tau_{rz} = G\left(\frac{\partial u}{\partial z} + \frac{\partial w}{\partial r}\right),$$

$$\sigma_z = 2G\left[\frac{\partial w}{\partial z} - \alpha\theta + \frac{\nu(\Theta - 3\alpha\theta)}{1 - 2\nu}\right] \tag{11}$$

when $B = 0$. Hence, Eq. (10) are reduced to the form analogous to (8) as follows

$$\overline{\nabla}^2\phi + 2(1 - \nu)Az - (1 + \nu)\alpha\theta = 0,$$

$$\nabla^2\theta + \frac{1}{\lambda}\frac{\partial\lambda}{\partial z}\frac{\partial\theta}{\partial z} = 0, \tag{12}$$

where $\overline{\nabla}^2 = \frac{1}{\partial r}\frac{\partial}{\partial}\left(r\frac{\partial}{\partial r}\right)$.

3 Example of application—thick plate made of FGM Al/ZrO$_2$+Y$_2$O$_3$

The general solution (12) can be written in a form, which is more suitable to plate problems, in which the thermoelastic solid is bounded by two parallel planes $x_3 = z = \pm h/2$ and exhibits axial symmetry

$$\frac{\partial^2\phi}{\partial r^2} + \frac{1}{r}\frac{\partial\phi}{\partial r} + 2(1 - \nu)Az - (1 + \nu)\alpha\theta = 0,$$

$$\frac{\partial^2\theta}{\partial r^2} + \frac{1}{r}\frac{\partial\theta}{\partial r} + \frac{\partial^2\theta}{\partial z^2} + \frac{1}{\lambda}\frac{\partial\lambda}{\partial z}\frac{\partial\theta}{\partial z} = 0. \tag{13}$$

Differentiation of Eq. (13$_1$) with respect to r and next substitution $u = \partial\phi/\partial r$, according to Eq. (9$_1$), leads to the classical Euler-type differential equation describing thermomechanical membrane state

$$\frac{\partial^2 u}{\partial r^2} + \frac{1}{r}\frac{\partial u}{\partial r} - \frac{u}{r^2} = (1 + \nu)\alpha\frac{\partial\theta}{\partial r}. \tag{14}$$

Unique solution of equation (14) that satisfies boundary conditions

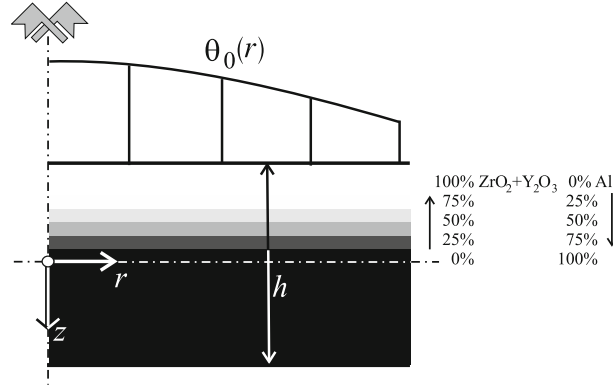$$u(0) = 0, \qquad \lim_{r\to\infty}\sigma_{r,\varphi} = 0, \tag{15}$$

takes form

$$u(r, z) = \alpha(z)\left[\frac{1 - \nu}{2}\theta(\infty) + \frac{1 + \nu}{r}\int_0^r \theta(\rho, z)\rho\,\mathrm{d}\rho\right]$$

$$\sigma_r(r, z) = E(z)\alpha(z)\left[\frac{\theta(\infty)}{2} - \frac{1}{r^2}\int_0^r \theta(\rho, z)\rho\,\mathrm{d}\rho\right]$$

$$\sigma_\varphi(r, z) = E(z)\alpha(z)\left[\frac{\theta(\infty)}{2} + \frac{1}{r^2}\int_0^r \theta(\rho, z)\rho\,\mathrm{d}\rho - \theta(r, z)\right], \tag{16}$$

Additionally, in case when temperature is bounded

$$\lim_{r\to\infty}\theta(r, z) = 0, \qquad \lim_{r\to\infty}\frac{1}{r^2}\int_0^r \theta(\rho, z)\rho\,\mathrm{d}\rho < \infty \tag{17}$$

Fig. 2 Three-layer thick plate made of FGM composite

Table 1 Selected properties of constituents of FGM after Wang et al. [14] and Lee et al. [15]

Constituent	E [GPa]	ν	λ [W/mK]	$\alpha \cdot 10^{-6}$ [1/K]
Al metal substrate	73	0.3	154	23
Al/$ZrO_2 + Y_2O_3$	205	–	2.0	9.8

solution (16) reduces to

$$u(r, z) = \alpha(z)\frac{1+\nu}{r}\int_0^r \theta(\rho, z)\rho\,\mathrm{d}\rho$$

$$\sigma_r(r, z) = -E(z)\alpha(z)\frac{1}{r^2}\int_0^r \theta(\rho, z)\rho\,\mathrm{d}\rho$$

$$\sigma_\varphi(r, z) = E(z)\alpha(z)\left[\frac{1}{r^2}\int_0^r \theta(\rho, z)\rho\,\mathrm{d}\rho - \theta(r, z)\right], \tag{18}$$

and it is clear that its dependence with respect to depth coordinate z comes from the functional gradation of Young's modulus $E(z)$ and thermal expansion coefficient $\alpha(z)$ as well the temperature field non-homogeneity $\theta(r, z)$ exclusively.

The boundary value problem, following example by Cegielski [13], is formulated as follows: find temperature distribution θ that fulfills Eq. (13_2) and boundary conditions

$$\theta(r, z)|_{z=-\frac{h}{2}} = \theta_0(r), \quad \left.\frac{\partial\theta(r, z)}{\partial r}\right|_{r=0} = 0$$

$$\left.\frac{\partial\theta(r, z)}{\partial z}\right|_{z=+\frac{h}{2}} = 0, \quad \int_{-\frac{h}{2}}^{+\frac{h}{2}} \lambda(z)\frac{\partial\theta(r, z)}{\partial r}\,\mathrm{d}z = \mathrm{const} \tag{19}$$

and accompanying plane stress components satisfying Eq. (18) for a semi-infinite axially symmetric three-layer thick plate made of FGM composite Al/ZrO_2 stabilized by Y_2O_3 (see Fig. 2).

The magnitudes of both materials being constituents of FGM, after Wang et al. [14] and Lee et al. [15], are presented in Table 1.

Let us assume that all thermomechanical properties of three-layer FGM depend on local magnitude of volume fraction of both constituents, which is subjected to the tangent hyperbolic approximation

$$p(z) = \frac{p_c + p_m}{2} + \frac{p_c - p_m}{2}\tanh(az + b) \tag{20}$$
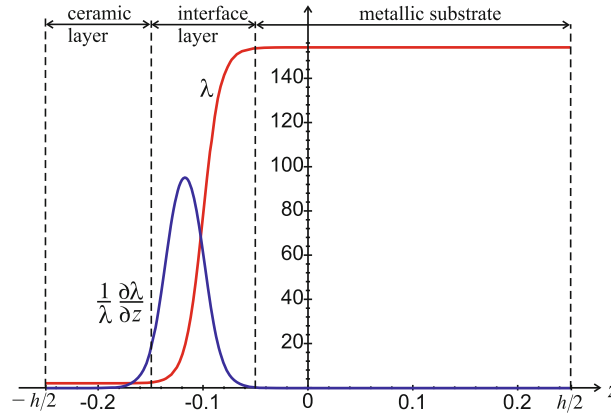
Fig. 3 Distributions of λ and $\frac{1}{\lambda}\frac{\partial\lambda}{\partial z}$
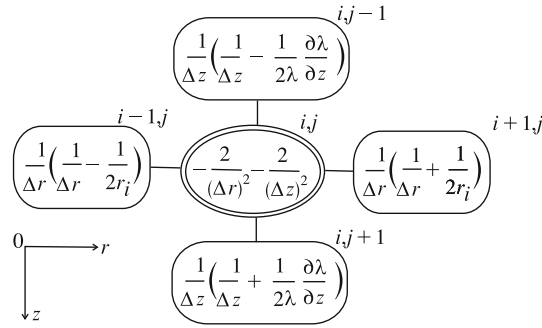
Fig. 4 Finite difference scheme for Fourier equation

where $p(z)$ stands for respective property $\lambda(z)$, $\alpha(z)$ or $E(z)$, indices "c" and "m" refer to ceramic or metallic materials, parameters a and b define location and thickness of interface layer. Differentiation of Eq. (20), next division it by $p(z)$ and finally substitution of $p_c = \lambda_c$ and $p_m = \lambda_m$, allows to easily find that coefficient of thermal non-homogeneity in Eq. (13_2) equals to

$$\frac{1}{\lambda}\frac{\partial\lambda}{\partial z} = \frac{\frac{\lambda_c+\lambda_m}{2}a\left[1 - \tanh^2(az + b)\right]}{\frac{\lambda_c+\lambda_m}{2} + \frac{\lambda_c-\lambda_m}{2}\tanh(az + b)} \tag{21}$$

Exemplary distributions of λ and $\frac{1}{\lambda}\frac{\partial\lambda}{\partial z}$ are shown in Fig. 3.

Applying finite difference method, one may perform Eq. (13_2) according to the scheme shown in Fig. 4, whereas appropriate schemes of boundary conditions allowing for elimination of nodes situated outside the domain are as follows

$$\theta_{i,j} = \theta_0(r) \quad z = -\frac{h}{2}, \quad \theta_{i,j+1} = \theta_{i,j-1} \quad z = \frac{h}{2},$$
$$\theta_{i-1,j} = \theta_{i+1,j} \quad r = 0, \quad \theta_{i+1,j} = \theta_{i-1,j} + 2\Delta_z g(z) \quad \text{sidewall} \tag{22}$$

The finite difference representation allows to substitute boundary value problem of partial differential equations by problem of searching for solution of a system of N linear equations involving N unknowns. This system of equations exhibits typical feature for sparse matrix system having relatively small number nonzero elements; hence, natural way to solve it is application of the row-indexed storage mode [16] combined with the conjugate gradient method [17].

Obviously, only small fragment, neighboring the axis of symmetry, of the whole infinite structure is considered. The finite difference operator, shown in Fig. 3, is spanned over the mesh of 161×81 square elements $\Delta r = \Delta z$. The thermal load applied to the upper surface of the plate is subjected to the following relation

$$\theta_0(r) = 300\left[1 - \tanh^2(2r)\right] \tag{23}$$
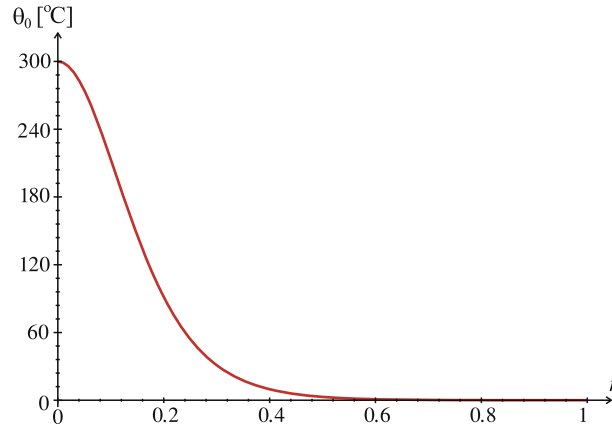
Fig. 5 Distribution of thermal load $\theta_0(r)$
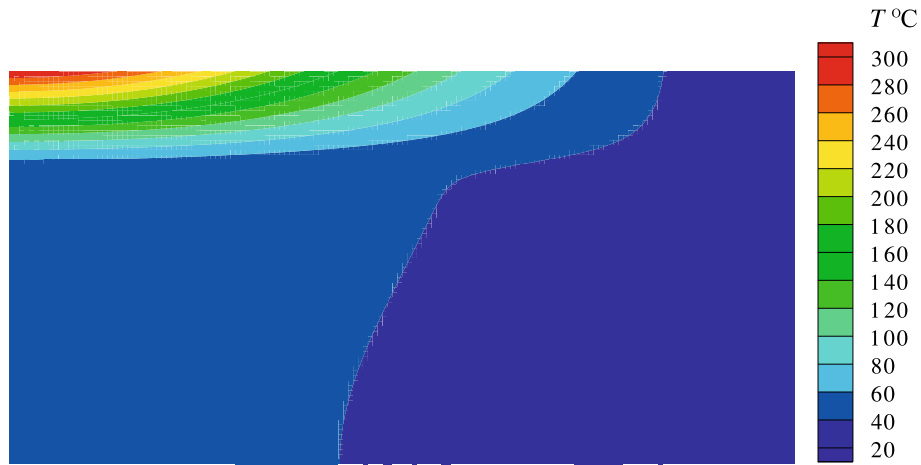
Fig. 6 Distribution of temperature field

which is illustrated in Fig. 5.

Temperature distribution is shown in Fig. 6. In comparison with the temperature distribution obtained for homogeneous material (see Cegielski [13]), the temperature field exhibits a drastic decrease in temperature at top layer. This is a consequence of application of ceramic material having coefficient of thermal conductivity 77 times lower than analogous coefficient of metallic substrate. Hence, one may clearly observe effect of thermal barrier coating with characteristic strong temperature gradients in it and simultaneous homogenization of temperature field in middle and bottom layers.

Aforementioned effect is more clearly visible in case of temperature gradient field $-\lambda\mathbf{grad}\theta$ presented in Fig. 7. The biggest magnitudes of temperature gradient, referring to top fibers of the plate, are almost 10 times bigger than analogous at bottom fibers.

Solution of mechanical problem is illustrated by distribution of hoop stress, which turns out to be the dominant component of stress, in Fig. 8. Analogously to the temperature field, application of functionally graded composite leads to the concentration of compressive stress in top layer being ceramic material of high toughness. This convenient effect is accompanied by simultaneous unloading of middle and bottom layers built of metallic substrate. Nevertheless, another effect of tensile stress zone in ceramic layer occurs. This phenomenon is strictly associated with the structure of equations defining stress components (18). Namely, as far as the radial stress is always negative, the hoop stress frequently changes sign, see Fig. 9.

Although due to continuity condition $\lim_{r\to 0}\sigma_r = \lim_{r\to 0}\sigma_\varphi$ both components take the same value $-E\alpha\theta(0)/2$ at the axis of symmetry and due to boundary conditions (15_2) they both approach zero at infinity, the hoop stress changes sign because term in square brackets in Eq. (18_3) is not always negative for all temperature functions of decreasing tendency.
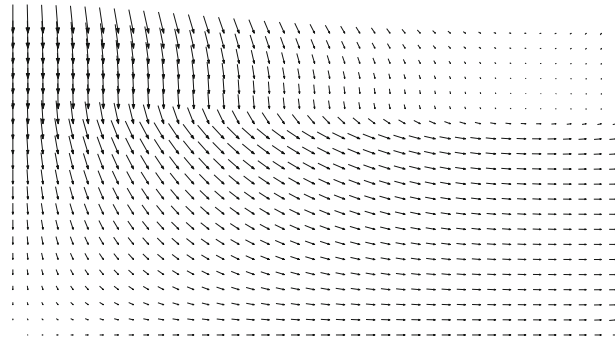
Fig. 7 Distribution of heat flux field

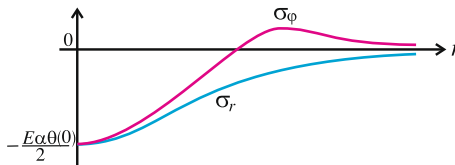**Fig. 8** Distribution of hoop stress field

Fig. 9 Typical distributions of radial and hoop stress components

As a consequence, a ceramic material of very low or zeroth tensile strength is obviously unable to carry tensile stress unless there exists residual stress built-in material, coming from fabrication process, big enough to neutralize tensile hoop stress. Otherwise, metal–ceramic FGM has to be replaced by metal–metal FGM, which exhibits sufficient tensile strength.

4 Conclusions

Following concluding remarks may be formulated for thick FGM plates.

- Thermal loading applied to the structure results in the plane stress state if only force-type boundary conditions are homogeneous and there are no body forces.
- There is no need to limit considerations to problems of specific power or exponential approximation functions since after application of Iljushin's potential only Fourier's equation turns out to have varying coefficient.
- Application of functionally graded composite $Al/ZrO_2+Y_2O_3$ is very efficient since FGM layer works like thermomechanical barrier, successively protecting metallic substrate from both high-temperature gradients and high concentration of compressive stress.

- Occurrence of tensile hoop stress in the ceramic layer is admissible only when it is accompanied be appropriate compressive residual stress.
- Both theorem and example of its application have only theoretical sense since neither manufacturing nor classical FEM does not allow for modeling of continuously varying FGM. Namely, from technological point of view the FGM interface layer deposed on top of metallic substrate exhibits hardly noticeable stress state, resulting form mismatch between metal and ceramic Young's modules and coefficients of thermal expansion. On the other hand, if the classical FEM is used for solving FGM problems, the material properties can only vary in a piecewise continuous manner since all integration points within an element have a common property value. To overcome this difficulty, a special graded element concept based on additional interpolation for nodal material properties is necessary to apply.

References

1. Noda, N.: Thermal stresses in functionally graded materials. J. Therm. Stress. **22**(4/5), 477–512 (1999)
2. Sneddon, I.N., Lockett, F.J.: On the steady- state thermoelastic problem for the half-space and the thick plate. Q. Appl. Math. **18**(2), 145–153 (1960)
3. Sternberg, E., McDowell, E.L.: On the steady-state thermoelastic problem for the half-space. Q. Appl. Math. **14**, 381 (1957)
4. Muki, R.: Thermal stresses in a semi-infinite solid and a thick plate under steady distribution of temperature. Proc. Fac. Eng. Keio Univ. **9**, 42 (1957)
5. Senthil, S.V., Batra, R.C.: Three-dimensional analysis of transient thermal stresses in functionally graded plates. Int. J. Solids Struct. **40**, 7181–7196 (2003)
6. Dai, K.Y., Liu, G.R., Han, X., Lim, K.M.: Thermomechanical analysis of functionally graded material (FGM) plates using element-free Galerkin method. Comput. Struct. **83**, 1487–1502 (2005)
7. Pan, E., Han, F.: Green's functions for transversely isotropic piezoelectric functionally graded multilayered half spaces. Int. J. Solid Struct. **42**, 3207–3233 (2005)
8. Wang, X., Pan, E., Roy, A.K.: Three-dimensional Green's functions for a steady point heat source in a functionally graded half-space and some related problems. Int. J. Eng. Sci. **45**, 939–950 (2007)
9. Jabbari, M., Shahryari, E., Haghighat, H., Eslami, M.R.: An analytical solution for steady state three dimensional thermoelasticity of functionally graded circular plates due to axisymmetric loads. Eur. J. Mech. A Solids **47**, 124–142 (2014)
10. Yang, K., Feng, W.-Z., Peng, H.-F., Lv, J.: A new analytical approach of functionally graded material structures for thermal stress BEM analysis. Int. Commun. Heat Mass Transf. **62**, 26–32 (2015)
11. Kulikov, G.M., Plotnikova, S.V.: A sampling method and its implementation for 3D thermal stress analysis of functionally graded plates. Compos. Struct. **120**, 315–325 (2015)
12. Iljushin, A.A., Lomakin, W.A., Shmakov, A.P.: Mechanics of Continuous Media, Moscow (1979)
13. Cegielski, M.: Numerical modeling of combustion engine piston made of MC composite. Diploma Thesis, Cracow University of Technology (2007)
14. Wang, B.L., Han, J.C., Du, S.Y.: Crack problems for functionally graded materials under transient thermal loading. J. Therm. Stress. **23**, 143–168 (2000)
15. Lee, W.Y., Stinton, D.P., Berndt, C.C., Erdogan, F., Lee, Y.-D., Mutasin, Z.: Concept of functionally graded materials for advanced thermal barrier coating applications. J. Am. Ceram. Soc. **79**, 3003–3012 (1996)
16. PCGPAK User's Guide, New Haven: Scientific Computing Associates Inc
17. Press, W.H., Teukolsky, S.A., Vetterling, W.T., Flannery, B.P.: Numerical Recipes in Fortran. Cambridge University Press, Cambridge (1983)